The high kinetic stability of a G-quadruplex limits hnRNP F qRRM3 binding to G-tract RNA

Brighton Samatanga[1,2], Cyril Dominguez[1], Ilian Jelesarov[2,*] and Frédéric H.-T. Allain[1,*]

[1]Department of Biology, Institute of Molecular Biology and Biophysics, ETH Zurich, CH-8093 Zurich, Switzerland and [2]Department of Biochemistry, University of Zurich, Winterthurerstrasse 190, CH-8057 Zurich, Switzerland

ABSTRACT

The RNA binding protein heterogeneous nuclear ribonucleoprotein (hnRNP) F is involved in telomeres maintenance and pre-mRNA processing, such as alternative splicing and polyadenylation. It specifically recognizes RNA containing three consecutive guanines (G-tracts) that have the potential to assemble into G-quadruplexes. We have proposed recently that hnRNP F could regulate alternative splicing by remodeling RNA structures, such as G-quadruplexes. However, the exact mechanism of hnRNP F binding to such RNA sequences remains unknown. Here, we have studied the binding of the third RNA binding domain of hnRNP F [quasi-RNA recognition motif 3 (qRRM3)] to G-tract RNA using isothermal titration calorimetry, circular dichroism and nuclear magnetic resonance spectroscopy. Our results show that qRRM3 binds specifically exclusively to single-stranded G-tracts (ssRNA), in contrast to previous reports stating that the G-quadruplex was recognized as well. Furthermore, we demonstrate that the pre-existent ssRNA/G-quadruplex equilibrium slows down the formation of the protein–ssRNA complex. Based on in vitro transcription assays, we show that the rate of the protein–RNA complex formation is faster than that of the G-quadruplex. We propose a model according to which hnRNP F could bind RNA co-transcriptionally and prevents G-quadruplex formation.

INTRODUCTION

Repeats of at least three consecutive guanines, known as G-tracts, have been shown to be over-represented in RNA molecules, especially near splice sites (1,2). These G-tracts play an important role in pre-mRNA alternative splicing by buffering splicing activity against 5′ splice site mutations (1). G-tracts have also been shown to be involved in the regulation of alternative splicing of several pre-mRNAs such as the thyroid hormone receptor (3), chicken cardiac troponin T (4) and the β-tropomyosin pre-mRNAs (5,6). G-tracts are therefore well-characterized cis-acting elements that often lead to exon inclusion or exclusion when positioned in the flanking introns or spliced exon, respectively (7). These G-rich cis-acting elements are specifically recognized by the heterogeneous nuclear ribonucleoprotein (hnRNP) F/H family of proteins that contain three quasi-RNA recognition motifs (qRRMs) and two Glycine-rich regions (8) (Supplementary Figure S1A). qRRMs differ from canonical RRMs by the lack of aromatics and basic residues in the conserved RNP1 and RNP2 sequences of RRM (9). We have recently solved the structures of each of the qRRMs of hnRNP F in complex with a G-tract containing RNA 5′-AGGGAU-3′ by solution nuclear magnetic resonance (NMR) spectroscopy (Supplementary Figure S1B) and observed that loop residues of the qRRM bind the RNA in a single-stranded form (ssRNA), despite the fact that the free RNA adopts a tetramolecular G-quadruplex fold (10). However, detailed kinetic and thermodynamic analysis of the effect of the G-quadruplex structure on complex formation was not investigated.

Recent studies have highlighted the importance of RNA structures in the regulation of alternative splicing [reviewed in (11)]. The over-representation of G-tracts in pre-mRNAs and their aptitude to participate in structure formation suggest that secondary structures, such as G-quadruplexes or stem-loops, are likely to form in vivo. Accordingly, it has been shown that G-quadruplex formation plays significant roles in many biological events such as transcription regulation (12,13), telomere biology (14), cancer biology (15), retroviral RNA dimerization (16) and mRNA processing (17,18). For example, it was shown that (UUAGGG)$_n$ repeat-containing telomeric RNA (19) can form G-quadruplexes in vivo (20–22), and that the RNA is bound and regulated by several hnRNP

proteins including hnRNP F that represses telomeric RNA expression (23). Furthermore, it has been shown by computational studies that C- and G-runs are over-represented upstream and downstream of exons, at conserved relative positions, suggesting that exon skipping may be achieved via a looping mechanism (24). In addition, numerous studies have provided *in vitro* evidence for the formation of G-quadruplexes under conditions mimicking the cellular environment (16,25). G-quadruplexes consist of stacked planes of G-tetrads stabilized by hydrogen bonds formed via the Hoogsteen faces of the guanine residues constituting a G-tetrad (Supplementary Figures S2A and S2B). Coordination by a central metal cation further stabilizes the structure. G-quadruplexes assemble in moderate salt concentrations. The kinetic and thermodynamic properties have been studied extensively in DNA molecules and in some RNAs (26–30). The association and dissociation processes are slow (27). They generally range from minutes to several days at physiological temperatures. Thus, as previously suggested on the basis of observed kinetic rate constants (16), a role for G-quadruplexes *in vivo* could be kinetically rather than thermodynamically driven. However, the kinetic and thermodynamic consequences of the slow rate of G-quadruplex unfolding on formation of protein–ssRNA complexes have never been fully investigated. This is the case despite the fact that numerous ssRNA binding proteins are known to bind G-quadruplex-forming sequences. In this context, hnRNP F is an interesting candidate because it has been argued that it can directly interact with quadruplexes (31,32). However, our previous structural studies provided evidence that hnRNP F binds only ssRNA and sequesters the guanines (10). Thus, we speculated that G-quadruplex formation could be prevented. To understand how the stability of G-quadruplex affects the thermodynamic and kinetic of protein binding, we have therefore studied the interaction of hnRNP F qRRM3 to a short G-tract RNA (AGGGAU) *in vitro* by a combination of microcalorimetry, circular dichroism (CD) and NMR spectroscopy. Our data indicate that the G-tract RNA exists as only two species, and the relative fractions depend on temperature. One specie corresponds to ssRNA and the other to a parallel G-quadruplex. Only the ssRNA is recognized by the protein. Dissociation of the quadruplex into ssRNA is independent from the presence of the protein. The dissociation is also characterized by a high activation energy barrier. The existence of this energy barrier explains why we observed a slow formation of the protein–ssRNA complex. We also show that a natural RNA substrate derived from the telomeric RNA adopts a highly stable G-quadruplex structure and does not bind to hnRNP F qRRM3. Moreover, using *in vitro* transcription assays, we show that hnRNP F qRRM3 can prevent G-quadruplex formation of the telomeric RNA by binding to ssRNA co-transcriptionally. These results have implications on the possible regulatory role of secondary structure formation in alternative splicing regulation and telomere biology, as well as on the mechanism of action of hnRNP F/H family of proteins in splicing and telomere maintenance.

MATERIALS AND METHODS

Oligonucleotides

HPLC-purified RNA oligonucleotides (5′-AGGGAU-3′ and 5′-AGG*G*AU-3′, where G* is 7-deazaguanine) were purchased from Metabion (Martinsried, Germany). GGA-(GGGUUA)$_4$ (TERRA1) and GAG-(UUAGGG)$_4$UUA (TERRA2) were transcribed *in vitro* by T7 polymerase from double-stranded DNA templates, and purified by anion-exchange HPLC. The concentration was determined by measuring the ultraviolet absorption at 260 nm. Because of the propensity of G-quadruplex formation, the concentration was determined after incubating the RNA at 90°C for at least 5 min from the absorption at 260 nm using extinction coefficients of 67 500 M^{-1}cm^{-1} for both AGG GAU and AGG*G*AU, 290 900 M^{-1}cm^{-1} for TERRA1 and 384 200 M^{-1}cm^{-1} for TERRA2. Samples containing quadruplexes were prepared by heating the RNA for 3–5 min at 98°C and incubating the samples at 4 (or 25)°C for several hours.

Protein expression and purification

qRRMs were expressed as previously described (33). The mass of the qRRMs was confirmed by either MALDI or ESI mass spectrometry. Ultraviolet absorption spectrometry was used for concentration determination. The extinction coefficient of qRRM3 was determined by amino acid analysis; ε = 12 000 M^{-1}cm^{-1}. The calculated extinction coefficient for qRRM12 was 16 500 M^{-1}cm^{-1}.

CD Spectroscopy

The CD spectra of free RNA, qRRM–RNA complexes and the *in vitro* transcription mixture were collected at 5–20 nm min^{-1} on a Jasco J-715 spectropolarimeter connected to a Julabo FS-18 temperature controller in quartz cuvettes of 2.00, 1.00 or 0.02-mm path length. Each spectrum was an average of 2–3 accumulations, except for the transcription mixture.

Isothermal titration calorimetry (ITC)

Isothermal titrations were conducted using a VP-isothermal titration calorimetry (ITC) microcalorimeter from GE Healthcare. ITC titrations were done at different temperatures (10°C, 18°C, 20°C, 25°C and 40°C) with different equilibration time between subsequent ITC injections (5 and 60 min) in sodium phosphate buffer (10 mM NaH$_2$PO$_4$ and 100 mM NaCl, pH 7.0) or in potassium phosphate buffer (10 mM KH$_2$PO$_4$ and 100 mM KCl, pH 7.0). The injection volume was ∼8.8 μl, and the reaction mixture was constantly stirred at 300 r.p.m. The concentration of reactants in the calorimetric cell or syringe was ∼10 μM and 150 μM, respectively.

NMR spectroscopy

The 1D ^{1}H and 2D ^{1}H-^{15}N heteronuclear single quantum correlation (HSQC) experiments were measured at 283, 298 and 313 K, respectively, on a Bruker DRX-750 MHz spectrometer. The qRRM3 concentration was between ∼0.2 mM for spectrum in the free state or bound to

RNA. Data were analyzed with Topspin 2.1 and Sparky software (http://www.cgl.ucsf.edu/home/sparky/).

Kinetics of G-quadruplex dissociation

The kinetics of dissociation of the G-quadruplex formed by AGGGAU RNA were followed by measuring the ellipticity at 265 nm wavelength as a function of time in sodium phosphate buffer at 25°C. The CD measurements were immediately started (within a dead time of ∼20 s) after adding a 2.7-μl aliquot of preformed 2.2 mM G-quadruplex stock into 297.3 μl of sodium phosphate buffer containing 0, 40 or 200 μM qRRM3. The final A GGGAU concentration was 20 μM. After correction for the instrumental baselines, the signal intensities were normalized to the range between 0 and 1 according to: $(S_t - S_{min})/(S_{max} - S_{min})$, where S_{max} and S_{min} are the maximum and minimum ellipticities, respectively, and S_t is the ellipticity measured at time t. The normalized data was then fitted with a first-order exponential decay equation of the form: $S_t = S_{amp} \exp(-t/\tau) + S_{eq}$, where S_{amp} and S_{eq} describe the amplitude and the final ellipticity (at equilibrium) of the dissociation curves, t is time and τ is the lifetime of the quadruplex. The dissociation rate constant, $k_{off} = 1/\tau$.

In vitro transcription

In vitro transcription assays were conducted at 37°C in the presence of different concentrations of qRRM3 (0, 20, 60 and 70 μM), 100 mM KCl and 40 mM NaCl, as well as 20 μM double-stranded DNA template, 40 μM MgCl₂, 5.8 mM of each of the four standard types of nucleotide triphosphates (NTPs) and 0.046 mg/ml T7 polymerase.

RESULTS

Thermodynamic profile of qRRM3 binding to G-tract RNA

HnRNP F contains three qRRM domains, each capable in itself of binding a G-tract RNA (10). Because hnRNP F qRRM3 is highly soluble and has the highest affinity for G-tract RNA, we decided to perform a thermodynamic profile of this RNA binding domain in complex with the G-tract RNA AGGGAU. To investigate the binding equilibrium between qRRM3 and AGGGAU, we performed ITC titrations at different temperatures in sodium phosphate buffer (10 mM NaH₂PO₄ and 100 mM NaCl, pH 7.0). At each temperature, the heat of reaction was measured after each injection of an aliquot of the RNA into the protein solution. At 40°C, successive injections of the RNA into the protein caused a progressive saturation of the available RNA binding sites described by a monophasic curve (Figure 1A, black curve). The transition point of the curve occurred at a molar ratio of 0.8. That is close to the one-to-one binding stoichiometry observed by NMR (10), assuming a 20% error in concentration determination. Binding isotherms obtained at lower temperatures showed two remarkable features: (i) there was a progressive transition from a monophasic behavior at 40°C to a biphasic character at lower

temperatures; and (ii) the stoichiometry of binding deviated from the expected value of one protein per RNA molecule. To better understand these deviations from simple binding equilibriums, we took into account the fact that for one-to-one binding systems, in the absence of accompanying equilibria, the choice of titrant and titrand should not influence the results. We, therefore, conducted reversed titrations by adding the protein into the RNA (Figure 1B). In this case, all the binding isotherms obtained were monophasic, but the stoichiometry of the complex increased with temperature (from 0.2 at 10°C to 0.8 at 40°C). As the results obtained in Figure 1A differ from those in Figure 1B, we confirm that the binding behavior is complicated by the presence of other equilibria. Three possible situations could explain this behavior: (i) the conformations of the protein and/or the RNA are temperature dependent; (ii) qRRM3 could also bind the G-quadruplex; and (iii) kinetic effects could overlap with the binding process. To eliminate the possibility of non-specific effects, blank experiments were performed by injecting RNA into buffer and buffer into protein. Only small heats because of mixing effects were observed that were insignificant in size relative to the binding signals (data not shown).

Effect of temperature on the conformations of G-tract RNA and qRRM3

Next, we investigated the temperature dependence of the conformations of the free protein and RNA. From the temperature dependence of the heat capacity measured by differential scanning calorimetry, we concluded that the free protein exists in its native state between 3°C and 50°C (Supplementary Figure S2A). The ITC studies fall within that temperature range, thus excluding the existence of temperature-dependent major conformational transitions in the protein. Further heating of the protein led to unfolding with a melting temperature (T_m) of 71.3°C. Next, we studied the temperature dependence of conformational transitions experienced by 100 μM G-tract RNA by CD spectroscopy in sodium phosphate buffer after incubating the G-tract at each temperature for several hours because equilibration is slow (27). The G-tract adopts a parallel four-stranded intermolecular G-quadruplex structure that is temperature dependent as revealed by a peak close to 265 nm and a trough at around 240 nm (34) (Figure 2A). The CD spectra at different temperatures cross-over at a single wavelength (isodichroic point). The isodichroic point is typically taken as evidence of the existence of only two molecular species (35). Therefore, these results strongly suggest that only the ssRNA and one type of G-quadruplex coexist in equilibrium. These results also imply that there are no transitions experienced between different G-quadruplex conformations in contrast to other G-tracts (36,37). Furthermore, the peak intensity at 265 nm increases with decreasing temperature indicating that larger fractions of G-quadruplexes are populated at lower temperatures. Because of this behavior and the occurrence of two saturation events (Figure 1A), we suspected that both ssRNA and the G-quadruplex might be recognized by qRRM3.
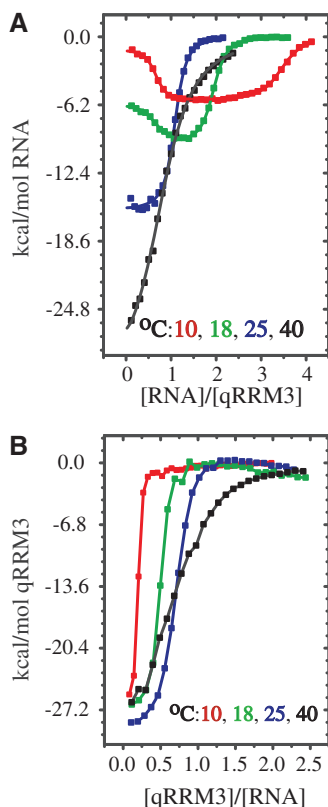
Figure 1. ITC binding isotherms between qRRM3 and G-tract RNA (**A**) Forward ITC titrations. Binding isotherms were obtained after injecting 150 µM 5′-AGGGAU-3′ into 10 µM qRRM3 in sodium phosphate buffer at different temperatures (as indicated in the figure). (**B**) Reversed ITC titrations. The binding isotherms were obtained after injecting 150 µM qRRM3 into 10 µM 5′-AGGGAU-3′ in sodium phosphate buffer at different temperatures, as indicated in the figure.

Interaction between qRRM3 and G-quadruplex RNA

To investigate whether qRRM3 can bind to G-quadruplexes, we performed ITC and NMR experiments under salt conditions that variably stabilize the G-quadruplex. The stability of G-quadruplexes is cation dependent. Potassium ions have a much higher stabilizing effect than sodium ions (38). Thus, we replaced the sodium phosphate buffer with potassium phosphate buffer (10 mM KH_2PO_4 and 100 mM KCl, pH 7.0). The T_m values of the G-quadruplexes obtained from thermal melting measurements by CD spectroscopy were 37.4°C and 73.0°C in the sodium and potassium phosphate buffers, respectively (Supplementary Figure S2B). However, the G-quadruplex still adopts the same conformation in both buffers below 20°C (Supplementary Figure S2C). From ITC binding isotherms obtained at 10°C in sodium phosphate buffer (Figures 1A and 2B, red curves), we observed large enthalpy changes when titrating the RNA into the protein. In contrast, only small signals exhibiting no saturation behavior were observed in potassium phosphate buffer demonstrating that qRRM3 cannot bind to the G-quadruplex (Figure 2B, black curve). This is contrasting with previous data that suggested a direct binding between hnRNP F and an

RNA G-quadruplex (31,32). To confirm our ITC data, we measured a ^{1}H-^{15}N heteronuclear single quantum correlation (HSQC) spectrum of the 1:1 mixture of qRRM3 and AGGGAU in potassium phosphate buffer at a concentration of 0.2 mM. We observed that the chemical shifts of the 1:1 mixture were similar to those of the free protein in solution (Supplementary Figure S2D). This similarity indicates that the presence of the G-quadruplex RNA did not perturb the molecular environment of the protein. Thus, these data provide further evidence for a lack of interaction between qRRM3 and a stable G-quadruplex RNA. Therefore, we speculated that the high kinetic stability of the G-quadruplex species could slow down the formation of the protein–ssRNA complex.

Kinetic effects of formation of the protein–ssRNA complex

To investigate the effects of kinetics on the formation of the protein–ssRNA complex, we performed ITC experiments at 20°C using different equilibration times between the successive injections of RNA into the protein (Figure 2C). Increasing the equilibration time from 5 to 60 min caused the binding isotherm to attain an almost monophasic character. Furthermore, the stoichiometry approached the expected value of one protein per RNA molecule confirming that the formation of the qRRM3–ssRNA complex is kinetically controlled. We speculated that the reason for slow complex formation is because of the presence of the G-quadruplex because dissociations of G-quadruplexes have been reported to be slow (27) (see also Figure 2E).

Characterization of G-quadruplex dissociation

Having concluded that qRRM3 did not bind G-quadruplex RNA, and that the presence of the G-quadruplex slowed down the formation of the protein–ssRNA complex, we investigated the rate of quadruplex dissociation in absence or presence of qRRM3. We measured the rate of G-quadruplex dissociation by a concentration jump experiment. This involved diluting the RNA 110-fold and immediately measuring changes in the CD intensity. The experiments were conducted as a function of time in sodium phosphate buffer at 265 nm wavelength and 25°C in the absence of qRRM3 (Figure 2D, black) and in its presence at different concentrations (Figure 2D, orange and green curves). We observed that the relaxation profiles were independent of protein concentration. Also, the final CD signal was lower in presence of protein than in its the absence (denoted by $\Delta\theta_{265}$; Figure 2D). These results indicate that qRRM3 simply sequesters the available ssRNA after intrinsic quadruplex dissociation. To confirm this, we normalized the CD signal from 0 to 1 to derive kinetic parameters (Figure 2E). The relaxation data were best described by a single exponential function. This is in agreement with the fact that G-quadruplex dissociation is a first-order process (27,30). The half-life values obtained at 2:1 and 10:1 excess of protein to G-tract were 35.8 and 27.4 min, respectively, demonstrating that the process is slow. The half-life of the dissociation of the free unbound quadruplex in the
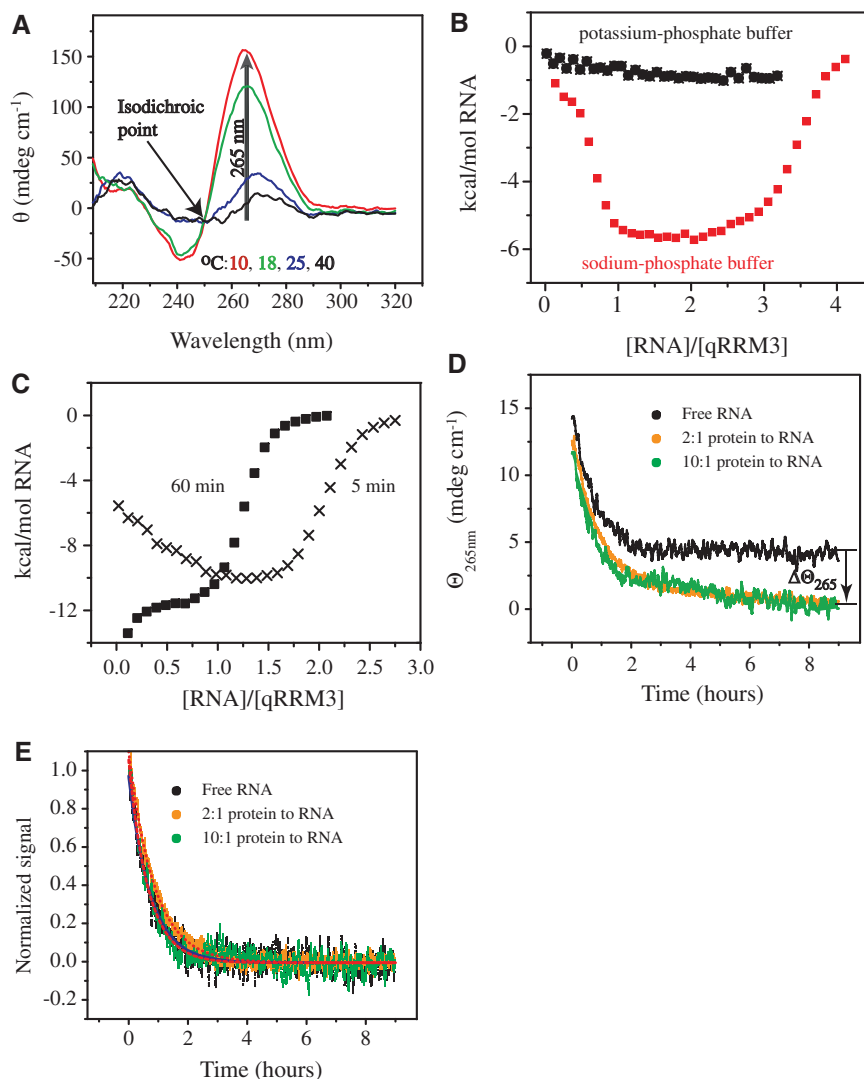
Figure 2. Binding of qRRM3 to G-tract RNA proceeds by conformational selection. (**A**) CD spectra of 100 μM 5′-AGGGAU-3′ measured in sodium phosphate buffer at different temperatures (indicated in the figure). (**B**) ITC binding curves measured at 10°C after injecting 150 μM 5′-AGGGAU-3′ into 10 μM qRRM3 in potassium phosphate buffer (black) and in sodium phosphate buffer (red). (**C**) ITC binding isotherms after titrating 150 μM 5′-AGGGAU-3′ into 10 μM qRRM3 at 20°C in sodium phosphate buffer with different equilibration time between successive injections amounting to 5 (crosses) and 60 min (squares). (**D**) CD time course measurements at 265 nm and 298 K showing the dissociation of G-quadruplex in the absence of qRRM3 (black), in a 2-fold excess of qRRM3 (40 μM; orange) and in a 10-fold excess of qRRM3 (200 μM; green) to RNA monomer (20 μM). The dead time was ~20 s. $\Delta\theta_{265}$ represents the change in G-quadruplex content at equilibrium due to the protein. (**E**) The figure shows the same data as in (**D**). The relaxation data was normalized from 1 (starting point) to 0 (final point). The solid blue line and the dotted and dashed red lines represent single exponential functions best describing the experimental data in the presence of 0, 40 and 200 μM qRRM3, respectively. The half-life of G-quadruplex dissociation is 30.5, 35.8 and 27.4 min for free G-quadruplex RNA and at 2- and 10-fold excess of protein to RNA, respectively.

absence of protein under the same conditions (Figure 2E, black curve) was similar (30.5 min). Therefore, the presence of protein does not lead to significant dissociation of the G-quadruplex. In conclusion, these results strongly demonstrate that the rate-limiting step for dissociation of the G-quadruplex is intrinsic, and the protein is not involved in that process.

Formation of the protein–ssRNA complex in the absence of G-quadruplexes

To understand the effect of the G-quadruplex on the formation of the protein–ssRNA complex, we studied the

binding equilibrium between the protein and the ssRNA species in the absence of G-quadruplexes. To eliminate the G-quadruplex population, we substituted the third and fourth guanines of AGGGAU with 7-deazaguanine to form deazaAGG*G*AU. The substitution of the N7 by a carbon in 7-deazaguanine (Figure 3A, inserted molecule) suppresses one hydrogen bond of the Hoogsteen base pair and has been shown to prevent G-quadruplex formation (39,40). Accordingly, the CD spectrum of deazaAGG*G*AU lacks a peak at around 265 nm or trough at 240 nm indicating that this oligomer does not populate G-quadruplexes compared with AGGGAU at a similar concentration (Figure 3A). This substitution
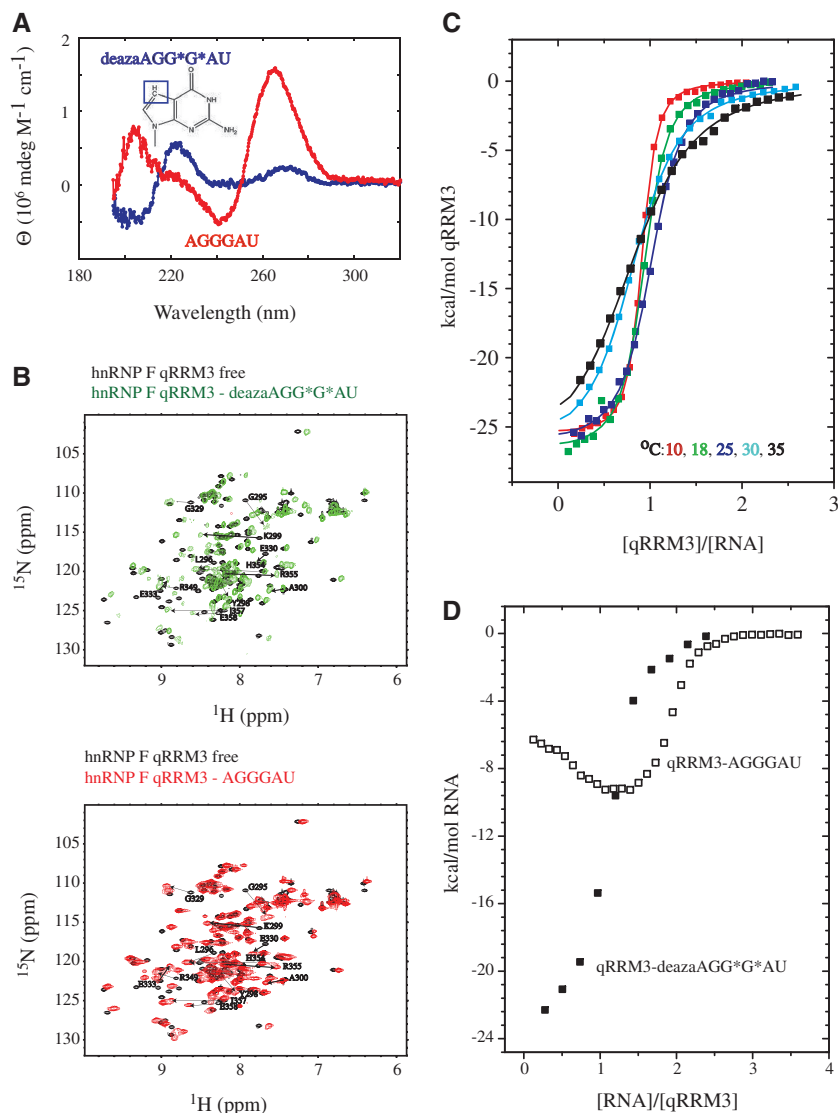
Figure 3. Binding of qRRM3 to single stranded G-tract RNA (**A**) CD spectrum of 5′-AGGGAU-3′ (red) and 5′-deazaAGG*G*AU-3′ (blue) in sodium phosphate buffer. The ′*′ represents 7-deazaguanine (inserted molecule). (**B**) Top: overlay of ^{1}H-^{15}N HSQC spectra of free qRRM3 (black) and qRRM3 in complex with 5′-deazaAGG*G*AU-3′ (green), Bottom: overlay of ^{1}H-^{15}N HSQC spectra of free qRRM3 (black) and qRRM3 in complex with 5′-AGGGAU-3′ (red). Spectra were determined at 20°C in 10–20 mM NaH$_2$PO$_4$, pH 7.0, with 36–50 mM NaCl with a qRRM3 concentration of 0.2 mM. (**C**) ITC binding curves after injecting 150 μM qRRM3 into 10 μM 5′-deazaAGG*G*AU-3′ in sodium phosphate buffer at different temperatures. (**D**) ITC binding curves after injecting 150 μM 5′-deazaAGG*G*AU-3′ (closed squares) and 5′-AGGGAU-3′ (open squares) into 10 μM qRRM3 at 18°C in sodium phosphate buffer.

should not affect the protein–RNA contacts because the N7 atoms of guanines 3 and 4 are not involved in hydrogen bonding with the protein (10). To confirm this, we measured a ^{1}H-^{15}N HSQC spectrum in sodium phosphate buffer of the complex formed between qRRM3 and deazaAGG*G*AU (Figure 3B, top) and compared the chemical shifts with those from the complex formed between qRRM3 and AGGGAU (Figure 3B, bottom). The similar chemical shift changes in both complexes indicate that the same binding surface of qRRM3 is involved in binding RNA. Therefore, the modification of the RNA does not significantly affect the binding to the protein. Next, we studied the binding equilibrium between qRRM3 and the deazaAGG*G*AU by ITC at different temperatures in sodium phosphate buffer (Figure 3C).

All binding curves are now monophasic. Also, the stoichiometry at all temperatures corresponds to one protein per RNA. This clearly indicates the absence of kinetic effects. Therefore, these experiments confirm that the presence of the G-quadruplex population slows down the formation of the protein–ssRNA complex. We next confirmed the binding model by switching between the titrant and titrand. Therefore, we instead injected deazaAGG*G*AU into qRRM3 at 18°C (Figure 3D). The binding isotherm obtained with the modified RNA is monophasic in contrast to the one previously observed with the unmodified RNA that can form a G-quadruplex. At 18°C, the averaged values for both the forward and reversed titrations between qRRM3 and deazaAGG*G*AU were 0.98 ± 0.02 for the stoichiometry and $0.18 \pm 0.02\ \mu M$ for

the dissociation constants (K_d). The two curves are super-imposable and conform to a simple one-to-one association reaction.

Interaction between qRRM3 and a long telomeric G-quadruplex

To understand the binding of hnRNP F to longer natural RNA substrates, we investigated the interaction between qRRM3 and G-tract RNA repeats consisting of >27 nt. For this purpose, we studied two natural RNAs: 5′-GGA-(GGGUUA)$_4$-3′ (TERRA1) and 5′-GAG-(UUAG GG)$_4$UUA-3′ (TERRA2). We refer to both sequences as TERRA. The two sequences differ in the starting point of the repeats (GGG or UUA). Except for the GGA or GAG overhangs required by T7 polymerase for efficient transcription initiation, the sequences correspond to telomeric RNA, which is bound by hnRNP F (23). The additional UUA at the 3′-end of TERRA2 was included to ensure the terminal guanine nucleotide is not cleaved off in the final product. The CD spectra of TERRA1 and TERRA2 are shown in Figure 4A (top) and Supplementary Figure S3A, respectively. The RNA spectra contain peaks at around 265 nm and troughs at around 240 nm indicating G-quadruplex formation (22,34). This is in agreement with the fact that TERRA sequence has been previously shown to form a unimolecular G-quadruplex (22). From CD thermal melting experiments measured in sodium phosphate buffer, we observed that TERRA1 exhibits high stability with a T_m >80°C (Figure 4A, bottom). The T_m for TERRA2 is the same confirming that the core structures formed by the TERRA sequences are the same (data not shown). The thermal stability of TERRA is similar to that observed in previous studies (22) further confirming the formation of G-quadruplexes. Interestingly, ITC binding isotherms on the interaction between qRRM3 and TERRA1 RNA measured at 40°C exhibited only partial stoichiometries indicating that the protein bound only to the ssRNA population (Figure 4B). This is in agreement with data obtained on AGGGAU at temperatures <25°C, where the G-quadruplex is stable (Figure 1B). In the titration of TERRA1 into the protein, the apparent stoichiometry is much larger than 1:1. In the titration of protein into TERRA, the apparent stoichiometry is much less than 1:1. These data are similar to the results obtained with AGGGAU RNA (Figure 1). Furthermore, the normalized heats between the titration of TERRA1 into protein and vice versa are about 3-fold different. This fact indicates the presence of other equilibria (in this case incomplete binding), as opposed to binding to the same species. Similar ITC data were obtained for the interaction between qRRM3 and TERRA2 (Supplementary Figure S3B). To further show that the G-quadruplex was not recognized, we measured CD spectra after titrating increasing concentrations of qRRM3 into 10 μM TERRA1 RNA at 40°C (Figure 4C). No shifts in the position or magnitude of the peak at around 265 nm were observed further confirming that qRRM3 cannot bind G-quadruplexes. The same behavior was observed during titration of qRRM3 into TERRA2 (Supplementary Figure S3C). In summary, these results

reinforce our initial finding that qRRM3 does not bind to G-quadruplexes, either monomeric or tetrameric. Furthermore, there was no significant change in the magnitude or position of the peak maxima of TERRA2 (Supplementary Figure S3D) on titrating the two-domain construct qRRM12 of hnRNP F (Supplementary Figure S1A) showing that even two tandem hnRNP F qRRMs cannot induce G-quadruplex dissociation.

Effect of qRRM3 on G-quadruplex formation

Because binding to ssRNA by qRRM3 cannot lead to significant G-quadruplex dissociation, we speculated that *in vivo,* hnRNP F might bind poly-G-tracts during transcription. Therefore, to explain the role of hnRNP F *in vivo*, we investigated the effect of qRRM3 on the formation of G-quadruplexes during *in vitro* transcription in the presence of 100 mM KCl and 40 mM NaCl using a T7 promoter (and T7 polymerase) and a double-stranded DNA template that can be transcribed into TERRA1 RNA. The *in vitro* transcriptions were performed at 37°C. The relative changes in the amount of G-quadruplexes formed were determined by CD spectroscopy (Figure 4D). We observed that the peak at around 265 nm decreased with increasing concentration of qRRM3 indicating the reduction in the amount of G-quadruplexes formed. Therefore, the presence of qRRM3 during transcription facilitated formation of the protein–ssRNA complex with consequent suppression of G-quadruplex formation. To confirm that the binding of qRRM3 to the RNA occurred co-transcriptionally, we performed an *in vitro* transcription assay in the absence of the protein and then incubated the mixture for 5–10 min with the protein (Figure 4E). As expected, the measured ellipticity remained the same confirming that the concentration-dependent effects of qRRM3 occurred during transcription of the RNA. To further confirm the effect of qRRM3 on G-quadruplex formation during transcription, we conducted two transcription assays, one in the presence of 70 μM qRRM3 and another in the absence of qRRM3 (0 μM qRRM3). Next, we probed for the presence of G-quadruplexes in the two assays using 30 mM NaOH (Supplementary Figure S4). Thirty millimolar NaOH has been shown to disrupt G-quadruplexes (29,41,42). Addition of 30 mM NaOH to the transcription mixture that contained no qRRM3 caused a decrease in the CD intensity at around 265 nm. No change was observed in the mixture containing 70 μM qRRM3. The decrease in peak intensity in the absence of protein indicated that G-quadruplexes were populated, in contrast to the sample containing qRRM3.

DISCUSSION

Mechanism of hnRNP F–G-quadruplex interaction

Despite several reports (31,32) indicating the existence of an interaction between hnRNP F/H family of proteins and G-tract RNAs, little is known about the mechanism of interaction. To our knowledge, this is the first study
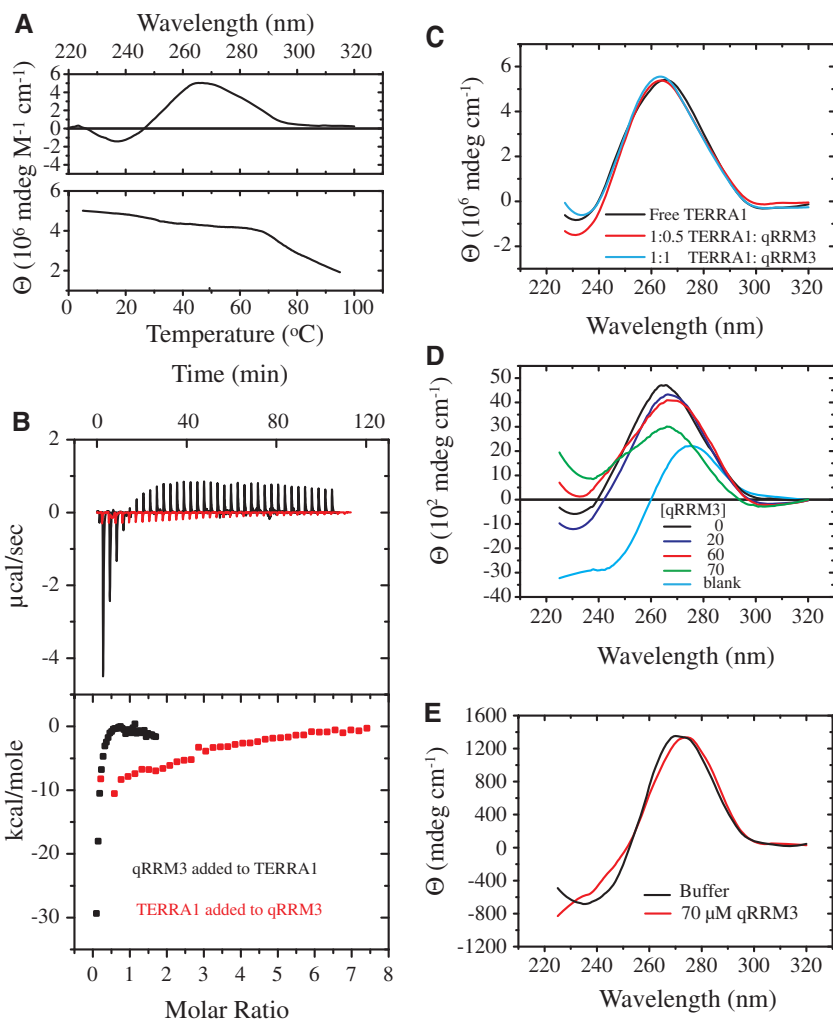
Figure 4. Interaction between qRRM3 and G-quadruplex formed by GGA-(GGGUUA)$_4$ (TERRA1) RNA (**A**) Top panel: CD spectrum of 5 μM 5′-GGA-(GGGUUA)$_4$-3′ (TERRA1) RNA measured at 25°C. Bottom panel: Thermal denaturation of 5 μM TERRA1 RNA determined by CD spectroscopy at 1°C min^{-1}. (**B**) ITC titrations conducted at 40°C in sodium phosphate buffer. In one case, 623 μM qRRM3 was titrated into 30 μM TERRA RNA (black). In the other case, 40 μM was titrated into 5 μM qRRM3 (red). The upper panel shows raw differential heat signals, whereas the lower panel shows the integrated and normalized data. (**C**) CD titration results on adding various concentrations of qRRM3 (0 μM, 20 μM and 40 μM) into 10 μM TERRA RNA at 40°C temperature in sodium phosphate buffer. The ratios are given in terms of the available binding sites (four sites per TERRA monomer) and not monomer concentrations. (**D**) CD spectra showing co-transcriptional effects. Effect of different concentrations of qRRM3 (indicated on figure) on the level of TERRA1 quadruplex after *in vitro* transcription (**E**) On termination of *in vitro* transcription assay with EDTA, either buffer (black) or 70 μM qRRM3 (red) was added followed by 5–10 min incubation at room temperature. All CDspectra were then collected at 37°C with a scan rate of 20 nm min^{-1}.

investigating how the equilibrium and kinetic effects of G-quadruplexes can affect G-tract RNA recognition by proteins. We investigated the interaction between qRRM3 and 5′-AGGGAU-3′ G-tract RNA by different techniques. The RNA sequence is part of the human immunodeficiency virus-1 p17gag instability sequence bound by hnRNP F (43). Solution NMR studies have shown that the RNA is sequestered in its single-stranded form (ssRNA) by qRRM3 (10). At the same time, CD studies have indicated that free G-tract RNA also populates a G-quadruplex conformation in the presence of 100 mM Na$^+$ or K$^+$ ions. Because of the distinctive spectral signatures of quadruplexes and ssRNA, and the presence of the isodichroic point in the CD spectra obtained at different temperatures, we concluded that 5′-AGGGAU-3′

populates only two species consisting of a parallel G-quadruplex in equilibrium with ssRNA. By using various techniques, we demonstrate here that qRRM3 interacts exclusively with ssRNA. ITC experiments with qRRM3 and 5′-AGGGAU-3′ showed no evidence of interaction in the presence of potassium ions, which are known to exert a large stabilization effect on the G-quadruplexes, the ssRNA being hardly populated in the tested concentration regime (Figure 2B). In the presence of sodium ions, there was interaction between the protein and the available small fraction of ssRNA. The conclusion that qRRM3 does not recognize the G-quadruplex is further reinforced by the fact that no significant chemical shift perturbations were observed by NMR on overlaying the spectra of the free protein and

that of 1:1 molar mixture of the protein and G-tract RNA in the presence of potassium ions (Supplementary Figure S2D). Additionally, the rates of G-quadruplex dissociation in the absence or in the presence of 2:1 and 10:1 excess of protein to RNA are nearly identical, providing further evidence for the lack of significant interaction between qRRM3 and G-quadruplex RNA (Figures 2D and E). In the presence of sodium ions, the stability of the quadruplex is lower, and a larger fraction of RNA adopts the single-stranded state. In these conditions, ITC binding isotherms showed progressive shifts from monophasic to biphasic behavior on a decrease in temperature (Figure 1A). Similarly, the apparent stoichiometry of binding markedly decreased from 40°C to 10°C. Although at first glance, this seems to suggest the existence of weak interactions between qRRM3 and the G-quadruplex, further experiments proved that this is not the case. In particular, by performing ITC experiments with longer equilibration time between successive injections, the biphasic behavior became monophasic, and the apparent stochiometry came in reasonable agreement with the expected 1:1 value obtained from structural studies (Figure 2C) (10). Therefore, the apparent biphasic behavior and partial stoichiometries reflect the slow kinetics of complex formation (protein–ssRNA) as dictated by the slow rate of G-quadruplex dissociation. If the protein indeed bound the G-quadruplex, binding would have been observed on performing the same experiments in the presence of potassium ions.

Partial stoichiometries were also observed during the interaction between qRRM3 and the G-quadruplexes formed by TERRA (TERRA1 or TERRA2) indicating that the protein cannot bind a natural G-quadruplex formed *in vivo* and cannot actively participate in its unfolding (Figure 4B and Supplementary Figure S3B). The experiments with TERRA were conducted in buffer containing sodium ions because the G-quadruplex already has high stability ($T_m > 80^\circ$C), which is greater than that of AGGGAU in the presence of potassium ions ($T_m = 73.0^\circ$C). In this way, any specific role of Na^+ or K^+ ions can be excluded. Titration of qRRM3 into TERRA RNA showed no evidence of shifts in the position or magnitude of the peak at around 265 nm, thus confirming that qRRM3 does not bind G-quadruplexes. This is consistent with the fact that the G-triplet is completely buried in the G-quadruplex fold (Figure 4C and Supplementary Figure S3C). Notably, all results collected here point to the lack of interaction between qRRM3 and the G-quadruplex, in contrast to previous studies that argue the existence of direct contacts between hnRNP F/H and a possible G-quadruplex structure located downstream of the p53 cleavage site (31). The different conclusions reached by Decorsiére *et al.* (31) are based on cross-linking and immunoprecipitation experiments. The choice of experimental conditions and the experimental setup, particularly the presence of other proteins, could possibly have played a role. We believe in providing, here, a more direct approach to the problem. The observed rates of dissociation obtained from CD experiments in our hands are comparable with those previously reported (27,30,44).

Differences in dissociation rates likely reflect the number of tetrads, the types of nucleic acid and the types and concentrations of salt ions present. To our knowledge, this is the first report on the dissociation kinetics of a G-quadruplex in the presence of a protein that functions by sequestering single-strand oligonucleotides by conformational selection from a pre-existing equilibrium. In this respect, the function of the protein or the nature of the equilibrium described in this manuscript is similar to the effect of a peptide nucleic acid trap on the unfolding of the quadruplex formed from human telomeric repeats (28). It is also similar to the effect of complimentary strands on unfolding of the quadruplex from the *Oxytricha* telomere DNA sequence (45). In our study, the obtained rate constant (k_{off}) of quadruplex dissociation is zero order with respect to the protein concentration, suggesting that the intrinsic opening and conformational rearrangement of the G-quadruplex is the rate limiting step, which is followed by a fast protein–ssRNA association. In agreement with this interpretation, fluorescence resonance energy transfer studies in 100 mM NaCl showed that a similar mechanism occurs in the unfolding transition of the intramolecular telomeric DNA quadruplex in the presence of a peptide nucleic acid trap (28). This further suggests that the rate-limiting step of G-quadruplex dissociation may be independent of the topology of the G-quadruplex.

Besides, by performing binding experiments by ITC using a 7-deazaguanine-modified oligonucleotide, we show that formation of the protein–ssRNA complex in the absence of G-quadruplex structure is characterized by a fast and simple one-to-one binding equilibrium at all temperatures (Figure 3). The destabilizing effect of 7-deazaguanine substitution on tetramolecular G-quadruplex DNA formation has been previously reported (39). It follows that the equilibrium population and the intrinsic kinetic stability of the quadruplex slow down the formation of the protein–ssRNA complex. In general, our results suggest that the overall equilibrium binding parameters (e.g. K_d) determined for the formation of complexes between ssRNA binding proteins and unmodified RNA containing G-tracts may be inaccurate, if the concentration of the binding-competent ssRNA species is not properly accounted for. Similarly to hnRNP F, other RNA binding proteins such as hnRNP A1, hPOT1 and hnRNP D have also been shown to bind RNA sequences forming G-quadruplexes (36,46–48). Interestingly, our binding model is in agreement with the inability of hnRNP A1 to unfold tetramolecular G-quadruplexes (46). However, hnRNP A1 has also been shown to play a role in the unfolding of telomeric DNA G-quadruplexes, exhibiting unimolecular and bimolecular topologies (36,46). The diverse effects of hnRNP A1 may reflect the extreme conformational diversity of telomeric DNA, which can form fold-back structures and consists of partially folded, short-lived and long-lived states (37). In fact, it has been demonstrated that hPOT1 does not bind telomeric DNA quadruplexes but may bind to partially folded states (14). Also, some of the nucleotides specifically recognized by hnRNP A1 and

hnRNP D (-UA-) remain exposed in their single-stranded form within loops intervening the G-tetrads (47–49). Weak interactions with partially exposed nucleotides most likely affect the G-quadruplex dissociation rate and stability, thereby explaining the effects on G-quadruplexes reported for those proteins. This is a key difference with hnRNP F that recognizes exclusively G-triplets and therefore could not bind to the TERRA RNA. Our data suggests that at least, in part, hnRNP A1, hnRNP D and hPOT1 might act similarly to hnRNP F by a conformational selection mechanism that sequesters available ssRNA that induces a slow reduction of the G-quadruplex population.

Function of hnRNP F *in vivo*

To address the function of hnRNP F *in vivo,* we investigated the interaction between qRRM3 and two natural telomeric G-tract RNAs, referred to as TERRA1 and TERRA2, which differ in the starting point of the repeats (GGG or UUA, respectively). These two TERRA-based RNA can form G-quadruplex structures as showed by the characteristic CD spectra with a peak at around 265 nm and trough at around 240 nm with thermal stability that is similar to that observed in previous studies (22). This is in further agreement with previous results showing that telomeric sequences can form G-quadruplexes both *in vitro* and *in vivo* (21,20). These TERRA G-quadruplexes are highly stable even in absence of K^+ ions (melting temperature $>80°C$ in presence of Na^+ ions). Our data indicates that qRRM3 cannot bind to G-quadruplexes formed by TERRA but only binds to the fraction of ssRNA available, in agreement to our data obtained on the short 5′-AGGGAU-3′ RNA. Consequently, qRRM3–ssRNA complex formation does not actively lead to G-quadruplex unfolding.

We further performed *in vitro* transcription experiments under conditions mimicking those found *in vivo* in the presence of various concentrations of qRRM3. We showed that the presence of increasing concentrations of qRRM3 during transcription causes a reduction of the amount of G-quadruplex formed, yet no reduction is observed on adding the protein at the end of the transcription assay (Figures 4D and E). Therefore, these results provide strong evidence that qRRM3 binds RNA co-transcriptionally, thus suppressing G-quadruplex formation. Consequently, we propose that any transcribed stretch of three guanines can be bound instantly by hnRNP F qRRMs before the entire strand is synthesized. In this way, the possible formation of intramolecular and intermolecular G-quadruplexes would be prevented. This model is in agreement with the fact that the formation of the protein–ssRNA complex is much faster than the association/dissociation kinetics of G-quadruplexes. The kinetics of quadruplex association/dissociation is likely to be even slower when considering the rates of RNA polymerase II (T7 polymerase). It has been argued that the effect of G-quadruplexes in the cell is most likely kinetic rather than thermodynamic (16). Furthermore, the suggestion that hnRNP F (and H) is observed at discrete locations in the nucleoplasm and acts at sites of transcription (8) offers support to our finding that hnRNP F binds ssRNA co-transcriptionally.

Although the results presented in this study have been obtained with the isolated qRRM3 domain, we would like to emphasize that the conclusions are applicable also to the function of full-length hnRNP F for the following reasons. First, we have shown previously by NMR that the qRRM domains tumble independently in solution (32). Furthermore, even the two-domain construct qRRM12 cannot induce significant dissociation of TERRA2 (Supplementary Figure S3D). Second, we have shown that isolated qRRM1 and qRRM3 domains mimic the function of full-length hnRNP F during alternative splicing of the Bcl-x RNA (10). Thirdly, evidence of co-transcriptional binding observed by using qRRM3 can only be strengthened by the use of full-length hnRNP F. The reason is that full-length hnRNP F consists of three qRRM domains, each capable of binding a G-tract, resulting in an increase of the local concentration of ssRNA binding sites (50) and a complex formation enhanced for kinetic and/or equilibrium reasons. This implies that significantly lower concentrations of hnRNP F are necessary to reproduce the effects obtained from the action of the isolated qRRM3. From a different perspective, the presence of potassium ions at higher concentrations and molecular crowding in cellular context (27,51) will both stabilize G-quadruplexes, and will thereby reinforce the interplay between the high kinetic stability of quadruplexes and the fast binding of ssRNA G-tracts as an important factor for modulating the biological function of hnRNP F, possibly also of other ssRNA binding proteins.

SUPPLEMENTARY DATA

Supplementary Data are available at NAR Online: Supplementary Figures 1–4.

ACKNOWLEDGEMENTS

FUNDING

Conflict of interest statement. None declared.

REFERENCES

1. Xiao,X., Wang,Z., Jang,M., Nutiu,R., Wang,E.T. and Burge,C.B. (2009) Splice site strength-dependent activity and genetic buffering by poly-G runs. *Nat. Struct. Biol.*, **16**, 1094–1100.

2. Wang,Z., Rolish,M.E., Yeo,G., Tung,V., Mawson,M. and Burge,C.B. (2004) Systematic identification and analysis of exonic splicing silencers. *Cell*, **119**, 831–845.

3. Hastings,M.L., Wilson,C.M. and Munroe,S.H. (2001) A purine-rich intronic element enhances alternative splicing of thyroid hormone receptor mRNA. *RNA*, **7**, 859–874.

4. Carlo,T., Sterner,D.A. and Berget,S.M. (1996) An intron splicing enhancer containing a G-rich repeat facilitates inclusion of a vertebrate micro-exon. *RNA*, **2**, 342–353.

5. Sirand-Pugnet,P., Durosay,P., Brody,E. and Marie,J. (1995) An intronic (A/U)GGG repeat enhances the splicing of an alternative intron of the chicken beta-tropomyosin pre-mRNA. *Nucleic Acids Res.*, **23**, 3501–3507.

6. Chen,C.D., Kobayashi,R. and Helfman,D.M. (1999) Binding of hnRNP H to an exonic splicing silencer is involved in the regulation of alternative splicing of the rat β-tropomyosin gene. *Genes Dev.*, **13**, 593–606.

7. Wang,Y., Ma,M., Xiao,X. and Wang,Z. (2012) Intronic splicing enhancers, cognate splicing factors and context-dependent regulation rules. *Nat. Struct. Biol.*, **19**, 1044–1052.

8. Matunis,M.J., Xing,J. and Dreyfuss,G. (1994) The hnRNP F protein: unique primary structure, nucleic acid-binding properties, and subcellular localization. *Nucleic Acids Res.*, **22**, 1059–1067.

9. Maris,C., Dominguez,C. and Allain,F.H.T. (2005) The RNA recognition motif, a plastic RNA-binding platform to regulate post-transcriptional gene expression. *FEBS J.*, **272**, 2118–2131.

10. Dominguez,C., Fisette,J.F., Chabot,B. and Allain,F.H. (2010) Structural basis of G-tract recognition and encaging by hnRNP F quasi-RRMs. *Nat. Struct. Biol.*, **17**, 853–861.

11. McManus,C.J. and Graveley,B.R. (2011) RNA structure and the mechanisms of alternative splicing. *Curr. Opin. Genet. Dev.*, **21**, 373–379.

12. Siddiqui-Jain,A., Grand,C.L., Bearss,D.J. and Hurley,L.H. (2002) Direct evidence for a G-quadruplex in a promoter region and its targeting with a small molecule to repress c-MYC transcription. *Proc. Natl Acad. Sci. USA*, **99**, 11593–11598.

13. Kumar,P., Yadav,V.K., Baral,A., Kumar,P., Saha,D. and Chowdhury,S. (2011) Zinc-finger transcription factors are associated with guanine quadruplex motifs in human, chimpanzee, mouse and rat promoters genome-wide. *Nucleic Acids Res.*, **39**, 8005–8016.

14. Zaug,A.J., Podell,E.R. and Cech,T.R. (2005) Human POT1 disrupts telomeric G-quadruplexes allowing telomerase extension in vitro. *Proc. Natl Acad. Sci. USA*, **102**, 10864–10869.

15. Gunaratnam,M., Fuente,M.dela, Hampel,S.M., Todd,A.K., Reszka,A.P., Schätzlein,A. and Neidle,S. (2011) Targeting pancreatic cancer with a G-quadruplex ligand. *Bioorg. Med. Chem.*, **19**, 7151–7157.

16. Sundquist,W.I. and Heaphy,S. (1993) Evidence for interstrand quadruplex formation in the dimerization of human immunodeficiency virus 1 genomic RNA. *Proc. Natl Acad. Sci. USA*, **90**, 3393–3397.

17. Marcel,V., Tran,P.L., Sagne,C., Martel-Planche,G., Vaslin,L., Teulade-Fichou,M.P., Hall,J., Mergny,J.L., Hainaut,P. and Van Dyck,E. (2010) G-quadruplex structures in TP53 intron 3: role in alternative splicing and in production of p53 mRNA isoforms. *Carcinogenesis*, **32**, 271–278.

18. Gomez,D., Lemarteleur,T., Lacroix,L., Mailliet,P., Mergny,J. and Riou,J. (2004) Telomerase downregulation induced by the G-quadruplex ligand 12459 in A549 cells is mediated by hTERT RNA alternative splicing. *Nucleic Acids Res.*, **32**, 371–379.

19. Azzalin,C.M., Reichenbach,P., Khoriauli,L., Giulotto,E. and Lingner,J. (2007) Telomeric repeat–containing RNA and RNA surveillance factors at mammalian chromosome ends. *Science*, **318**, 798–801.

20. Randall,A. and Griffith,J.D. (2009) Structure of long telomeric RNA transcripts the G-rich rna forms a compact repeating structure containing G-quartets. *J. Biol. Chem.*, **284**, 13980–13986.

21. Xu,Y., Suzuki,Y., Ito,K. and Komiyama,M. (2010) Telomeric repeat-containing RNA structure in living cells. *Proc. Natl Acad. Sci. USA*, **107**, 14579–14584.

22. Martadinata,H., Heddi,B., Lim,K.W. and Phan,A.T. (2011) Structure of Long Human Telomeric RNA (TERRA): G-quadruplexes formed by four and eight UUAGGG repeats are stable building blocks. *Biochemistry*, **50**, 6455–6461.

23. de Silanes,I.L., d' Alcontres,M.S. and Blasco,M.A. (2010) TERRA transcripts are bound by a complex array of RNA-binding proteins. *Nat. Commun.*, **1**, 1–9.

24. Miriami,E., Margalit,H. and Sperling,R. (2003) Conserved sequence elements associated with exon skipping. *Nucleic Acids Res.*, **31**, 1974–1983.

25. Xu,Y., Kimura,T. and Komiyama,M. (2008) Human telomere RNA and DNA form an intermolecular G-quadruplex. *Nucleic Acids Symp. Ser.*, **52**, 169–170.

26. Hardin,C.C., Perry,A.G. and White,K. (2000) Thermodynamic and kinetic characterization of the dissociation and assembly of quadruplex nucleic acids. *Biopolymers*, **56**, 147–194.

27. Lane,A.N., Chaires,J.B., Gray,R.D. and Trent,J.O. (2008) Stability and kinetics of G-quadruplex structures. *Nucleic Acids Res.*, **36**, 5482–5515.

28. Green,J.J., Ying,L., Klenerman,D. and Balasubramanian,S. (2003) Kinetics of unfolding the human telomeric DNA quadruplex using a PNA trap. *J. Am. Chem. Soc.*, **125**, 3763–3767.

29. Mergny,J.L., De Cian,A., Ghelab,A., Saccà,B. and Lacroix,L. (2005) Kinetics of tetramolecular quadruplexes. *Nucleic Acids Res.*, **33**, 81–94.

30. Wyatt,J.R., Davis,P.W. and Freier,S.M. (1996) Kinetics of G-quartet-mediated tetramer formation. *Biochemistry*, **35**, 8002–8008.

31. Decorsière,A., Cayrel,A., Vagner,S. and Millevoi,S. (2011) Essential role for the interaction between hnRNP H/F and a G quadruplex in maintaining p53 pre-mRNA 3′-end processing and function during DNA damage. *Genes Dev.*, **25**, 220–225.

32. Fisette,J.F., Montagna,D.R., Mihailescu,M.R. and Wolfe,M.S. (2012) A G-Rich element forms a G-quadruplex and regulates BACE1 mRNA alternative splicing. *J. Neurochem.*, **121**, 763–773.

33. Dominguez,C. and Allain,F.H. (2006) NMR structure of the three quasi RNA recognition motifs (qRRMs) of human hnRNP F and interaction studies with Bcl-x G-tract RNA: a novel mode of RNA recognition. *Nucleic Acids Res.*, **34**, 3634–3645.

34. Paramasivan,S., Rujan,I. and Bolton,P.H. (2007) Circular dichroism of quadruplex DNAs: applications to structure, cation effects and ligand binding. *Methods*, **43**, 324–331.

35. Juban,M.M., Javadpour,M.M. and Barkley,M.D. (1997) Circular dichroism studies of secondary structure of peptides. *Methods Mol. Biol.*, **78**, 73–78.

36. Krüger,A.C., Raarup,M.K., Nielsen,M.M., Kristensen,M., Besenbacher,F., Kjems,J. and Birkedal,V. (2010) Interaction of hnRNP A1 with telomere DNA G-quadruplex structures studied at the single molecule level. *Eur. Biophys. J.*, **39**, 1343–1350.

37. Lee,J.Y., Okumus,B., Kim,D.S. and Ha,T. (2005) Extreme conformational diversity in human telomeric DNA. *Proc. Natl Acad. Sci. USA*, **102**, 18938–18943.

38. Hud,N.V., Smith,F.W., Anet,F.A.L. and Feigon,J. (1996) The Selectivity for K+ versus Na+ in DNA quadruplexes is dominated by relative free energies of hydration: a thermodynamic analysis by 1 H NMR. *Biochemistry*, **35**, 15383–15390.

39. Gros,J., Rosu,F., Amrane,S., De Cian,A., Gabelica,V., Lacroix,L. and Mergny,J.-L. (2007) Guanines are a quartet's best friend: impact of base substitutions on the kinetics and stability of tetramolecular quadruplexes. *Nucleic Acids Res.*, **35**, 3064–3075.

40. Benimetskaya,L., Berton,M., Kolbanovsky,A., Benimetsky,S. and Stein,C.A. (1997) Formation of a G-tetrad and higher order structures correlates with biological activity of the RelA (NF-κB p65) 'antisense' oligodeoxynucleotide. *Nucleic Acids Res.*, **25**, 2648–2656.

41. Arimondo,P.B., Riou,J.F., Mergny,J.L., Tazi,J., Sun,J.S., Garestier,T. and Hélène,C. (2000) Interaction of human DNA topoisomerase I with G-quartet structures. *Nucleic Acids Res.*, **28**, 4832–4838.

42. Lyonnais,S., Hounsou,C., Teulade-Fichou,M., Jeusset,J., Cam,E.L. and Mirambeau,G. (2002) G-quartets Assembly Within a G-rich DNA Flap. *A Possible Event at the Center of the HIV-1 Genome. Nuceic Acids Res.*, **30**, 5276–5283.

43. Caputi,M. and Zahler,A.M. (2001) Determination of the RNA Binding Specificity of the Heterogeneous Nuclear Ribonucleoprotein (hnRNP) H/H′/F/2H9 Family. *J. Biol. Chem.*, **276**, 43850–43859.

44. Petraccone,L., Erra,E., Randazzo,A. and Giancola,C. (2006) Energetic aspects of locked nucleic acids quadruplex association and dissociation. *Biopolymers*, **83**, 584–594.

45. Raghuraman,M.K. and Cech,T.R. (1990) Effect of monovalent cation-induced telomeric DNA structure on the binding of oxytricha telomeric protein. *Nucleic Acids Res.*, **18**, 4543–4552.

46. Fukuda,H., Katahira,M., Tsuchiya,N., Enokizono,Y., Sugimura,T., Nagao,M. and Nakagama,H. (2002) Unfolding of quadruplex structure in the G-rich strand of the minisatellite repeat by the binding protein UP1. *Proc. Natl Acad. Sci. USA*, **99**, 12685–12690.

47. Nagata,T., Kurihara,Y., Matsuda,G., Saeki,J., Kohno,T., Yanagida,Y., Ishikawa,F., Uesugi,S. and Katahira,M. (1999) Structure and interactions with RNA of the N-terminal UUAG-specific RNA-binding domain of hnRNP D0. *J. Mol. Biol.*, **287**, 221–237.

48. Enokizono,Y., Konishi,Y., Nagata,K., Ouhashi,K., Uesugi,S., Ishikawa,F. and Katahira,M. (2005) Structure of hnRNP D complexed with single-stranded telomere DNA and unfolding of the quadruplex by heterogeneous nuclear ribonucleoprotein D. *J. Biol. Chem.*, **280**, 18862–18870.

49. Ding,J., Hayashi,M.K., Zhang,Y., Manche,L., Krainer,A.R. and Xu,R.M. (1999) Crystal structure of the two-RRM domain of hnRNP A1 (UP1) complexed with single-stranded telomeric DNA. *Genes Dev.*, **13**, 1102–1115.

50. Kuriyan,J. and Eisenberg,D. (2007) The origin of protein interactions and allostery in colocalization. *Nature*, **450**, 983–990.

51. Miyoshi,D., Karimata,H. and Sugimoto,N. (2007) Hydration regulates the thermodynamic stability of DNA structures under molecular crowding conditions. *Nucleosides. Nucleotides. Nucleic. Acids*, **26**, 589–595.